

# A Study on EMI Noise Countermeasure Design of a Dishwasher

Soongkeun Lee, Changdae Joo  and Taekue Kim \* 

Department of Electric Engineering, Changwon National University, Changwon 51140, Republic of Korea; 20177566@gs.cwnu.ac.kr (S.L.); ckd422@naver.com (C.J.)

\* Correspondence: tkkim@changwon.ac.kr; Tel.: +82-55-213-3633

**Abstract:** In this paper, we introduce and propose a design strategy implemented to mitigate electro-magnetic interface (EMI) issues arising from the switching circuitry of dishwashers, encompassing components such as inverters and switched-mode power supplies (SMPSs). The focus lies on addressing conducted emissions (CEs) by analyzing the impedance of the load and core characteristics at the current level to implement enhancements. Additionally, we describe the incorporation of a common mode (CM) core attachment design aimed at the resonance frequency of the motor, effectively blocking noise generated by this resonant frequency and thereby enhancing radiated power (RP). Also, we discuss the modeling of noise filters and the overall system, comparing impedance characteristics, and validating the effectiveness of the proposed improvements through standardized tests. Furthermore, practical application to mass-produced products is demonstrated by eliminating internal harness cores and designing noise filters to reduce their size, all within the context of dishwasher EMI countermeasures.

**Keywords:** EMI; dishwasher; CE; RP; EMI core; filter; EMI countermeasures design



**Citation:** Lee, S.; Joo, C.; Kim, T. A Study on EMI Noise Countermeasure Design of a Dishwasher. *Electronics* **2024**, *13*, 94. <https://doi.org/10.3390/electronics13010094>

Academic Editors: Alistair Duffy and Gang Zhang

Received: 27 November 2023

Revised: 20 December 2023

Accepted: 20 December 2023

Published: 25 December 2023



**Copyright:** © 2023 by the authors. Licensee MDPI, Basel, Switzerland. This article is an open access article distributed under the terms and conditions of the Creative Commons Attribution (CC BY) license (<https://creativecommons.org/licenses/by/4.0/>).

## 1. Introduction

The EMC regulations in various countries around the world are continuously strengthening, and companies are highly responsive to EMC regulations for product sales [1,2]. For household appliances, the applicable regulations vary by country, but are generally based on CISPR 14-1 and FCC Part 18. In the case of Korea, CISPR 14-1 is followed, and for EMI (electro-magnetic interface), compliance with Table 1 is required for CE (conducted emission) and RP (radiated power). Various improvement measures are applied to develop household appliances in compliance with EMC standards. However, the most common and easily applicable method is to implement a CM (common mode) core by applying ferrite cores to the harness. Nevertheless, this method has the main drawback of increasing costs and the complexity of the product, even though it offers the advantage of short-term noise improvement. Companies are making various efforts to eliminate ferrite cores. However, due to various factors such as the wiring of the product, the material of the cover, PCB artwork, etc., the noise characteristics change, making it difficult to accurately determine the final form of the noise. Initially, only the main noise frequencies are addressed, and if specification failures occur in the final test, hardware developers resort to easily implementable methods, such as adding ferrite cores to the harness for noise reduction, as structural and PCB changes are often not feasible. Therefore, in this paper, we examine the noise characteristics of motors, considered as the main noise sources in household appliances, and explore countermeasures.

### 1.1. Differentiation According to Noise Paths

The noise generated during the on/off operation of the power switch is categorized into two types based on the transmission path of the noise. Firstly, differential mode refers to the voltage measured between the power lines (live/neutral) or the current flowing through the two lines [3]. This current flows only through the power lines without returning

through the ground, ultimately resulting in the difference between the V1 and V2 lines. The transmission path of differential mode noise is illustrated in Figure 1. In this case, only the pure differential mode voltage, determined by the difference between V1 and V2, and the differential mode current, determined by the load impedance, flow through the load. Typically, the differential mode current flowing through the load is the current considered during circuit design and is used for the normal circuit functionality implementation. Therefore, the differential mode signal is also referred to as the normal mode signal.

**Table 1.** Limit of conducted emission (CE) and radiated power (RP).

	Frequency (MHz)	Limit	
		Quasi-Peak	Average
Conducted Emission (dBuV)	0.15~0.5	66~56 *	56~46 *
	0.5~5	56	46
	5~30	60	50
Radiated Power (dBpW)	30~300	45~55	35~45

\* Decreases with logarithm of frequency.

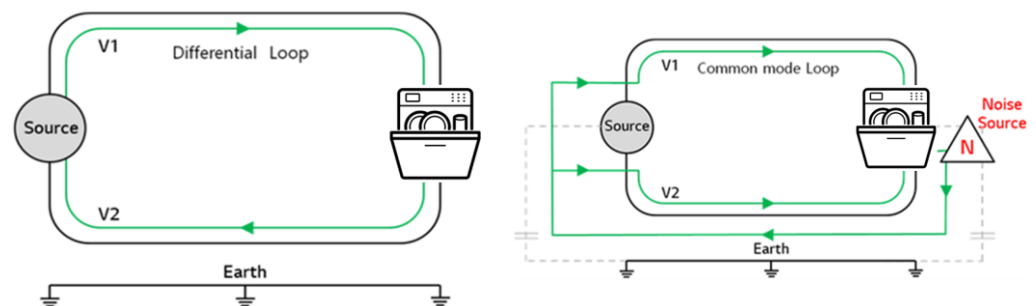


**Figure 1.** Noise paths of differential mode and common mode.

Common mode noise is the current or voltage measured between the power line and ground. It refers to the case where currents in the V1 and V2 lines flow in the same direction. In this scenario, noise requires a return path, and a current path is formed through parasitic capacitance generated between the circuit and ground, allowing the current to flow through the ground. To explain this in more detail, both V1 and V2 have the same common mode voltage, and through parasitic capacitance, common mode current flows into the ground. As the differential mode voltage is 0, no current flows to the load. Typically, common mode current flowing into the ground is considered unwanted by circuit designers and represents noise current unrelated to normal circuit functionality [4].

### 1.2. EMI Countermeasures According to Noise Modes

Generally, noise reduction methods include damping methods using coils and bypass methods using capacitors. As explained in Section 1.1, since the transmission paths of noise differ depending on the noise mode, the countermeasures for noise suppression also vary according to the noise mode.

In this section, we would like to explain EMI countermeasure methods according to the mode. Firstly, for common mode noise, as the noise flows along the ground path, to attenuate the noise it is necessary to design a coil that can generate inductance when noise flows in the same direction at node 1 and node 2, as shown in Figure 2. This approach is called a common mode choke. In Figure 3, we have briefly illustrated the form of application of the common mode choke and the resulting attenuation of noise when applied. Additionally, in Figure 3, to bypass common mode noise, capacitors directly connected to ground from V1 and V2 are represented.

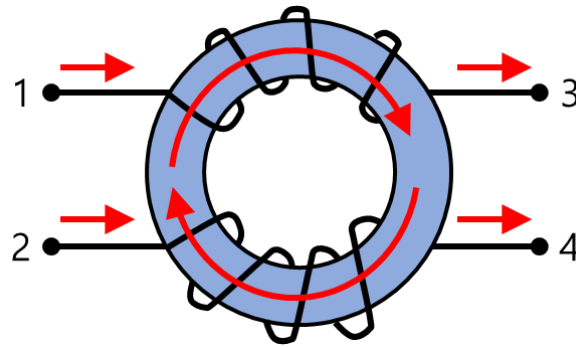


Figure 2. Common mode choke current direction and core internal magnetic flux direction.

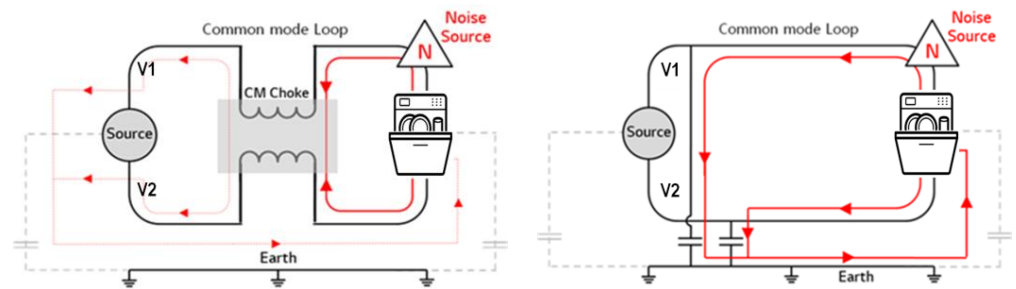


Figure 3. Common mode choke and Y-capacitor to reduce common mode noise.

Secondly, for differential mode noise, since V1 and V2 flow in opposite phases, to mitigate noise a coil should be designed such that when noise flows in different directions in nodes 1 and 2 (Figure 4) an inductance can occur. This method is called a differential mode choke. In Figure 5, we briefly illustrate the form of application and the shape of noise attenuation when applied. Additionally, in Figure 5, to bypass the differential mode noise, a capacitor directly connecting V1 to V2 is represented.

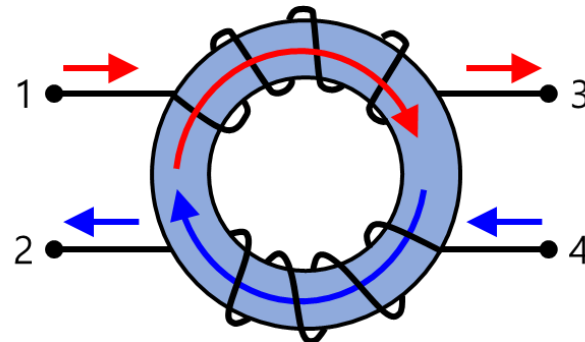


Figure 4. Current direction in differential mode choke and magnetic flux direction inside the core.

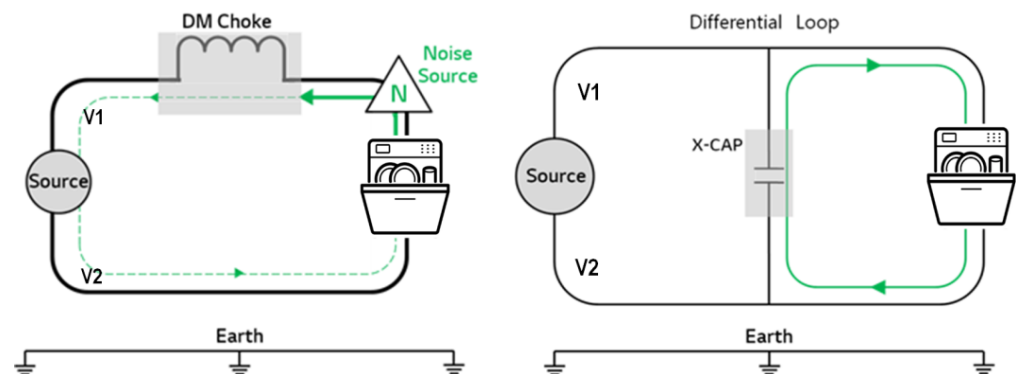
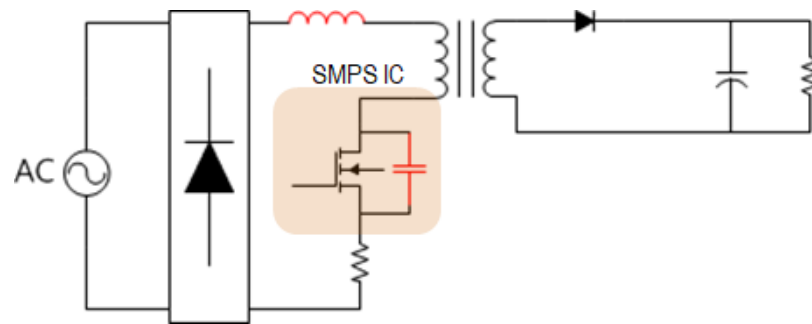


Figure 5. Differential mode choke and X-capacitor to reduce differential mode noise.

### 1.3. Noise Shape in Switched-Mode Power Supply (SMPS)

The primary power supply used for driving DC loads in household appliances is typically a flyback SMPS (switched-mode power supply) with a power rating of 100 W or less. In the case of a flyback SMPS, momentary voltage spikes occur during the power switch's off state, leading to the generation of noise through high-frequency paths [4].

Figure 6 illustrates the parasitic inductance and capacitance that form the high-frequency path, and to assess the noise, the actual PCB was used to measure the power switch terminals (Vds), as shown in Figure 7 [5].



**Figure 6.** Expression of parasitic inductance and parasitic capacitance becoming high-frequency path in flyback converter.

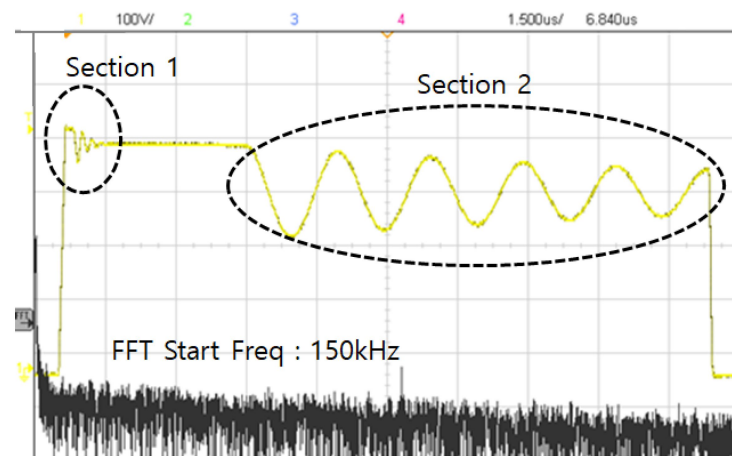


**Figure 7.** Vds measurement waveform and FFT results of power switch in flyback converter.

Due to ringing phenomena occurring in Sections 1.1 and 1.3, EMI components were observed at 450 kHz and 5 MHz in the FFT results. However, for SMPS, common EMI countermeasures, such as the RCD snubber, are typically applied. We have presented the FFT results for CM and DM noise and SMPS switching noise in Figure 8. The actual EMI measurement results in Figure 9 did not show significant differences due to SMPS operation [6,7]. Therefore, this paper focuses on the analysis of motor drive noise in the dishwasher.

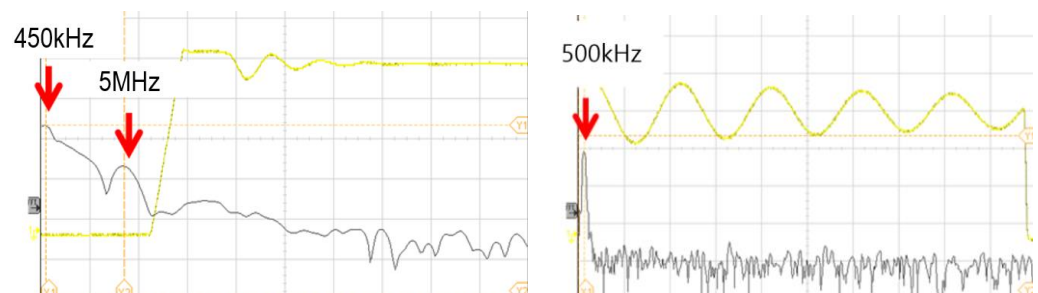


**Figure 8.** FFT results for CM and DM noise and SMPS switching noise.

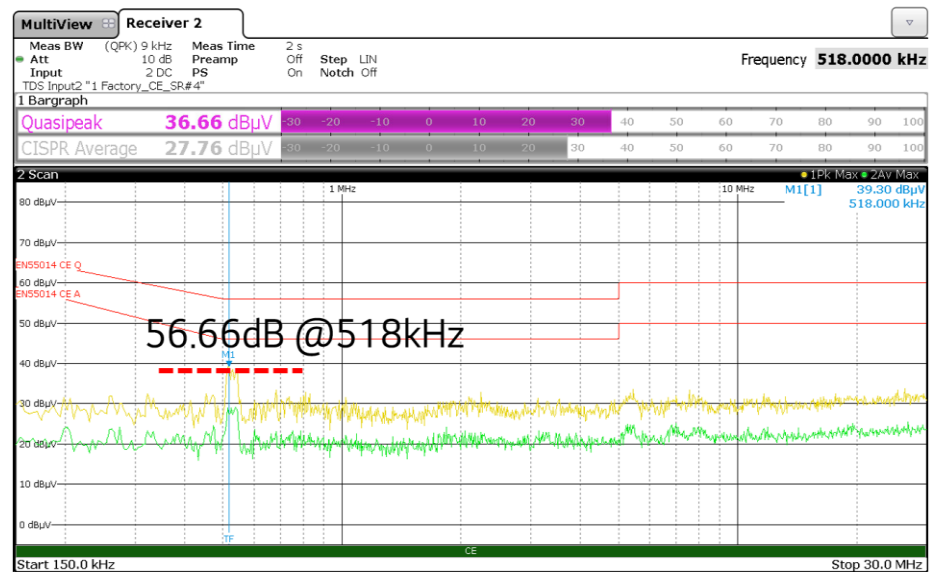


Figure 9. Noise results after driving SMPS.

#### 1.4. Discussion

This paper discusses the improvement of noise sources in a dishwasher (Model: Dishwasher Steam Freestanding 12-person capacity) by applying harness cores and explores EMI countermeasure design techniques. For conducted emission (CE), an impedance analysis was conducted using an impedance analyzer to analyze the impedance of loads such as washing motors, drainage motors, and heaters. After characteristic analysis, improvements were made to the filters and cores to enhance the CE performance.

To suppress noise due to the resonance frequency of the washing motor, a common mode (CM) core designed for the resonance band was implemented on the printed circuit board (PCB). Subsequently, simulations were performed considering the washing motor and power input lines, and an EMI countermeasure design was implemented by optimizing the noise filter for radiated power (RP). Meanwhile, the application of a common mode core effectively reduced the overall system noise. However, due to the bulk design of the existing noise filter, lightweighting of the noise filter became necessary. Therefore, the rationale for noise filter lightweighting and the design approach were derived based on simulations and subsequently validated through experiments. In other words, initial efforts were directed towards realizing a reduction in the overall system noise, followed by the design of the noise filter, based on a simulation analysis for size reduction, and validation through experiments.

## 2. Analysis of EMI Phenomena in Dishwashers

To analyze and derive improvement directions for accurate EMI countermeasure design, the current EMI levels (CE, RP) were measured with the existing EMI design removed. Additionally, to identify EMI countermeasure directions, measurements were taken for the common mode (CM) and differential mode (DM) [8,9].

### 2.1. Analysis of a Dishwasher's EMI (CE, RP)

To assess the current EMI levels, CE and RP were measured with the EMI countermeasures (harness core, noise filter) removed, and the results are shown in Figure 10.

As indicated in Figure 10, for CE, a maximum improvement of 45dBµV is required in the frequency range of 150 kHz to 20 MHz, and for RP, a maximum improvement of 19 dBpW is needed in the frequency range of 30 MHz to 40 MHz.

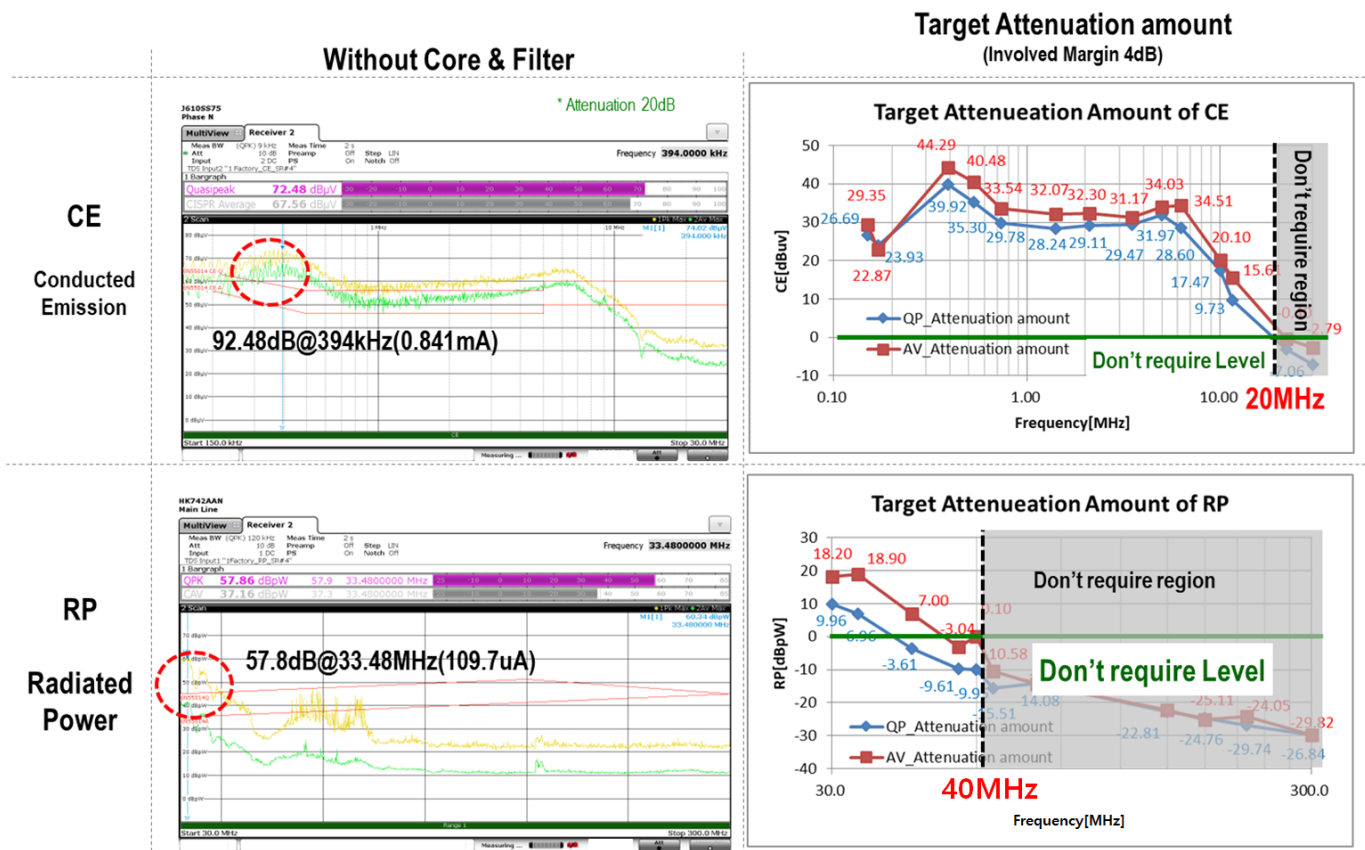


Figure 10. CE and RP with EMI countermeasures removed and target attenuation amount of CE and RP.

### 2.2. Analysis of a Dishwasher’s EMI (CM, DM)

We analyzed the CE of EMI and divided it into CM and DM after removing the EMI countermeasures, and the results are shown in Figure 11. The measurement results indicated the need for simulation measures for CM and DM noise at 150 kHz. In the frequency range up to ~30 MHz, it was observed that the CM values were larger than the DM values, and the maximum target attenuation was measured at 51 dBuV@362 kHz. Considering that CM noise dominates in the target model, it was determined that EMI countermeasures are needed by identifying the path of noise leakage from the load first [10,11]. For CM components, this is generated due to the loop between ground and the power supply. A typical form of ground core is applied to the main load (washing motor) of the dishwasher product. The current location of the harness core is shown in Figure 12.

We present the common impedance of the washing motor connected to the product’s ground and the EMI results of CE in Figure 13. Examining the common impedance of the washing motor in Figure 13, resonance is observed at 450 kHz and 11 MHz, and it was confirmed that the actual EMI values are much higher in these frequency ranges. Additionally, the major noise paths of the entire system, as shown in Figure 12, are schematically represented in Figure 14 [12].

Meanwhile, the common impedance of the motor can be considered to be caused by the impedance due to the parasitic capacitance between the stator winding and ground, as shown in Figure 15.

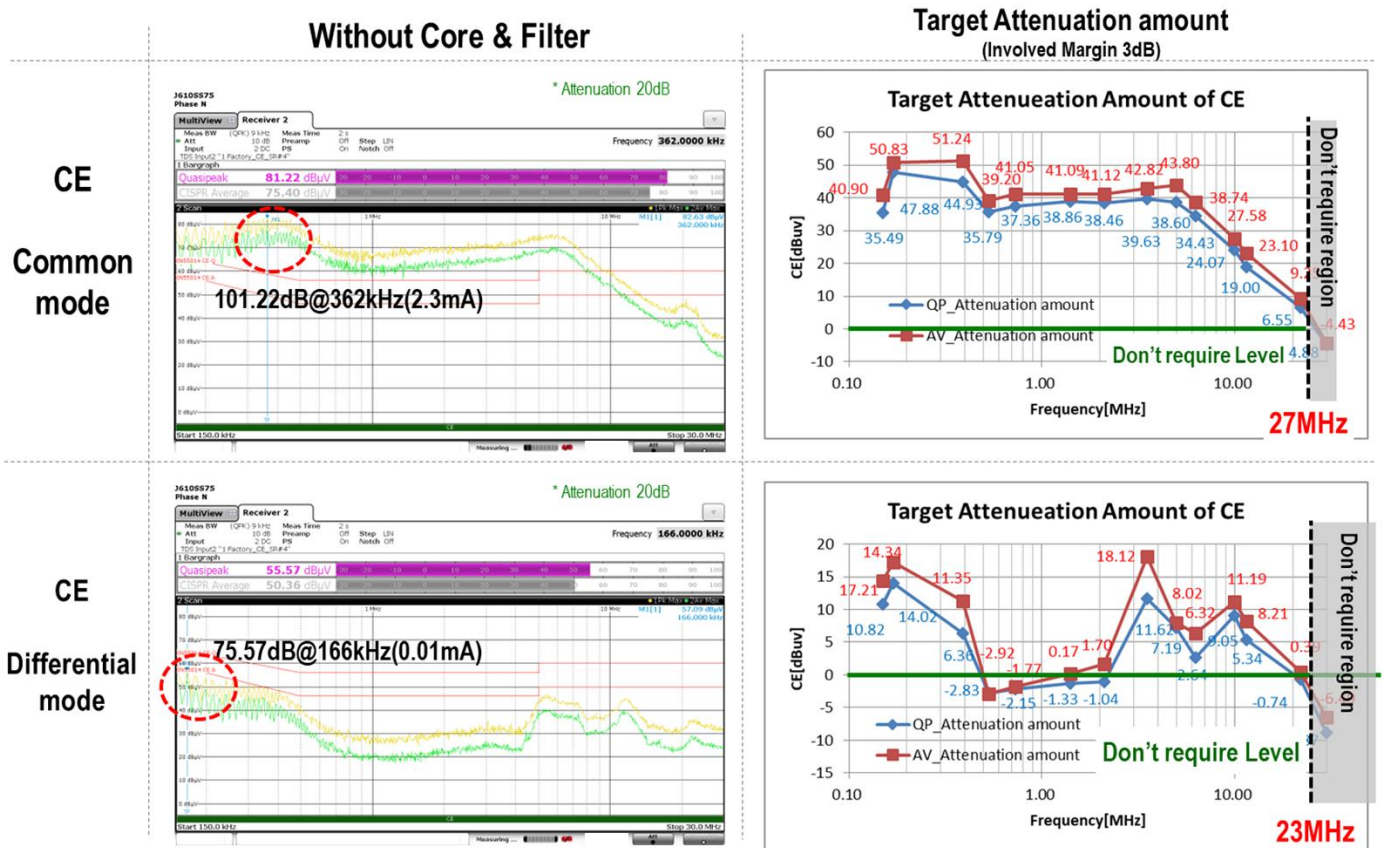


Figure 11. CM and DM with EMI countermeasures removed.

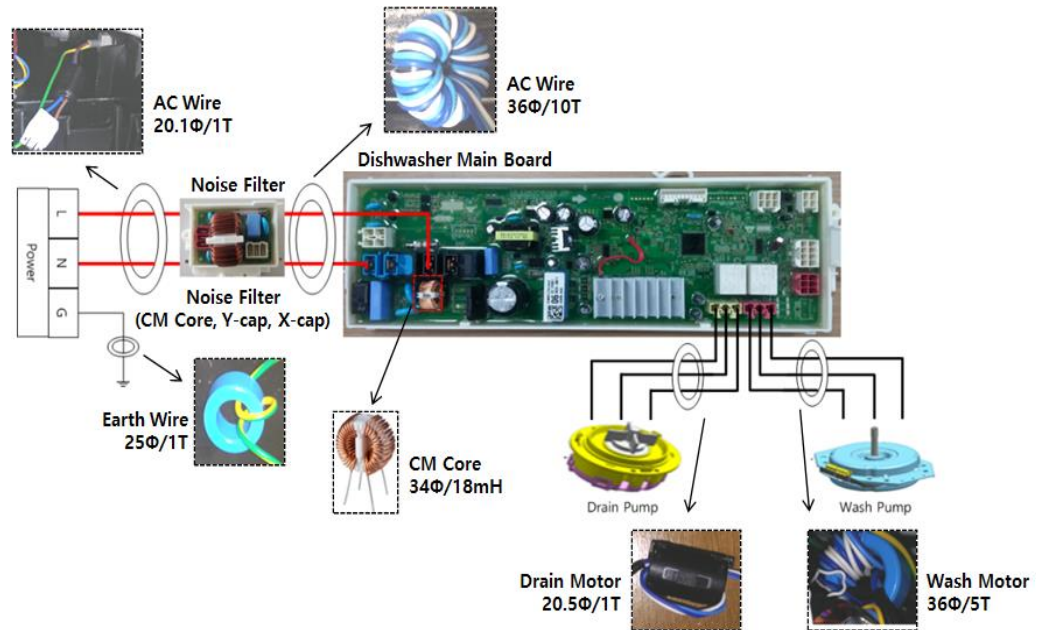


Figure 12. Location of the core designed inside the product.

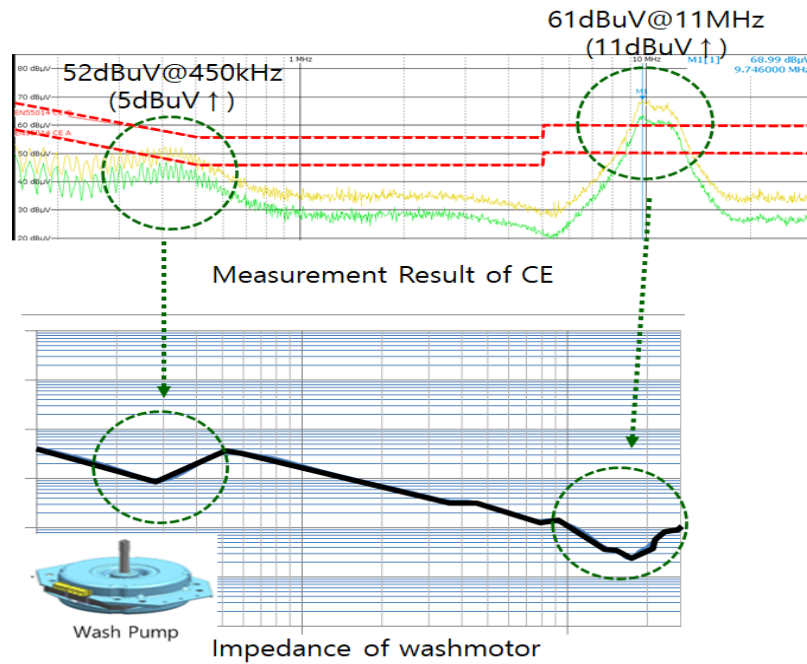


Figure 13. Relationship between the impedance of the washing motor and the CE results.

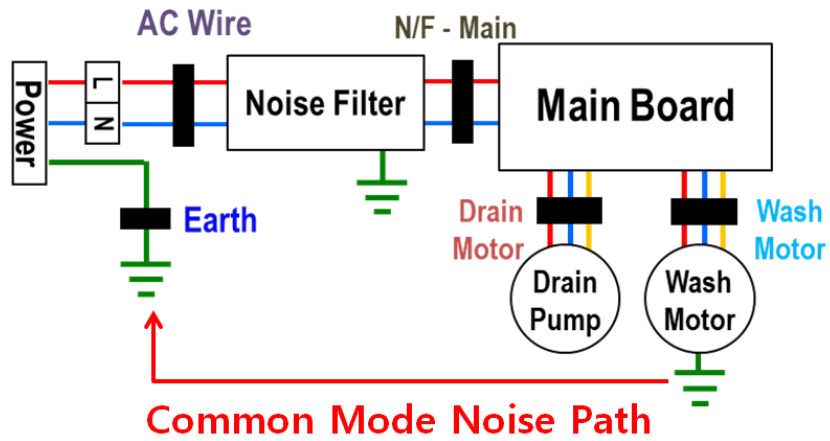


Figure 14. Dominant noise path in entire system.

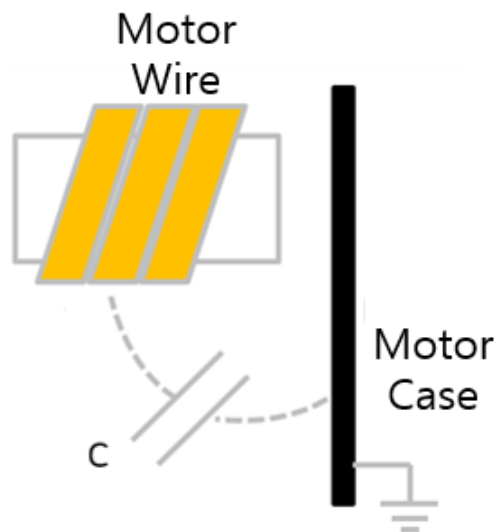


Figure 15. Parasitic capacitance occurring in the motor windings and motor case.

This parasitic capacitance can vary depending on the motor's shape or winding method. Referring to the literature, assuming the motor's shape is the same, it was confirmed that the resonance frequency varies according to the motor's winding method (delta or star winding). For star winding [13], resonance occurs in the 50 kHz range, while for delta winding, it occurs in the 300 kHz range.

In Figure 13, the actual EMI values represent the noise difference after removing the ferrite core applied to the harness of the washing motor. The measured CE results show an increase of approximately 5 dBuV at 450 kHz, reaching 52 dBuV, and an increase of about 11 dBuV at 11 MHz, reaching 61 dBuV. This indicates that to improve the noise from the washing motor's CM component, measures should be taken with a high-impedance core (large diameter and many turns) at 450 kHz and 11 MHz.

Therefore, in this paper, leveraging the occurrence of EMI noise at the washing motor's common mode impedance resonance frequency, noise countermeasures were implemented proactively in the product design based solely on the motor information, as shown in Table 2. To attenuate EMI noise, a 3-phase common mode core was designed to increase the impedance of the filter, aligning it with the resonance frequency of 450 kHz.

**Table 2.** Application of EMI countermeasures and summary of improvements according to design method.

	Improvement after EMI Measurement		Improvement before EMI Measurement
	Noise Filter Design	3 Phase Core Design	3 Phase Core Design
Design Method	Using insertion loss Calculate Load Impedance	Using Parameter Modeling	Using load resonance Calculate Target Frequency

### 2.3. CE Analysis According to Operating Conditions

While operating the product under various loads, an analysis of unfavorable EMI conditions was conducted for each load, and the results are illustrated in Figures 16 and 17. In the CE domain, there was no deviation during the main PCB assembly power on/off, but an increase was observed. When operating the WOW motor, there was an increase of 36 dBuV at 300 kHz and 31 dBuV at 6.7 MHz.

Furthermore, due to the drain motor drive, there was an increase of 29.6 dBuV and 33 dBuV in the same frequency range. In the RP domain, there was a 4 dBuV increase during main PCB Assembly power activation, while during the washing motor operation, there was an increase of 15.4 dBuV, and during the drain motor operation, a 24.2 dBuV increase was observed at 40 MHz.

### 2.4. Attenuation Characteristics Analysis for EMI (CE) Improvement

For mass production EMI countermeasures, the attenuation characteristics of each core and noise filter applied were analyzed using an impedance analyzer (E4990A, Keysight) and practical measurements. The characteristics of the relevant cores are illustrated in Figure 18.

Based on these results, three harness cores, excluding the noise filter, were applied for CE improvement, while two harness cores were applied for RP improvement. Therefore, it was determined that integration of harness cores responsible for the same frequency band is necessary.

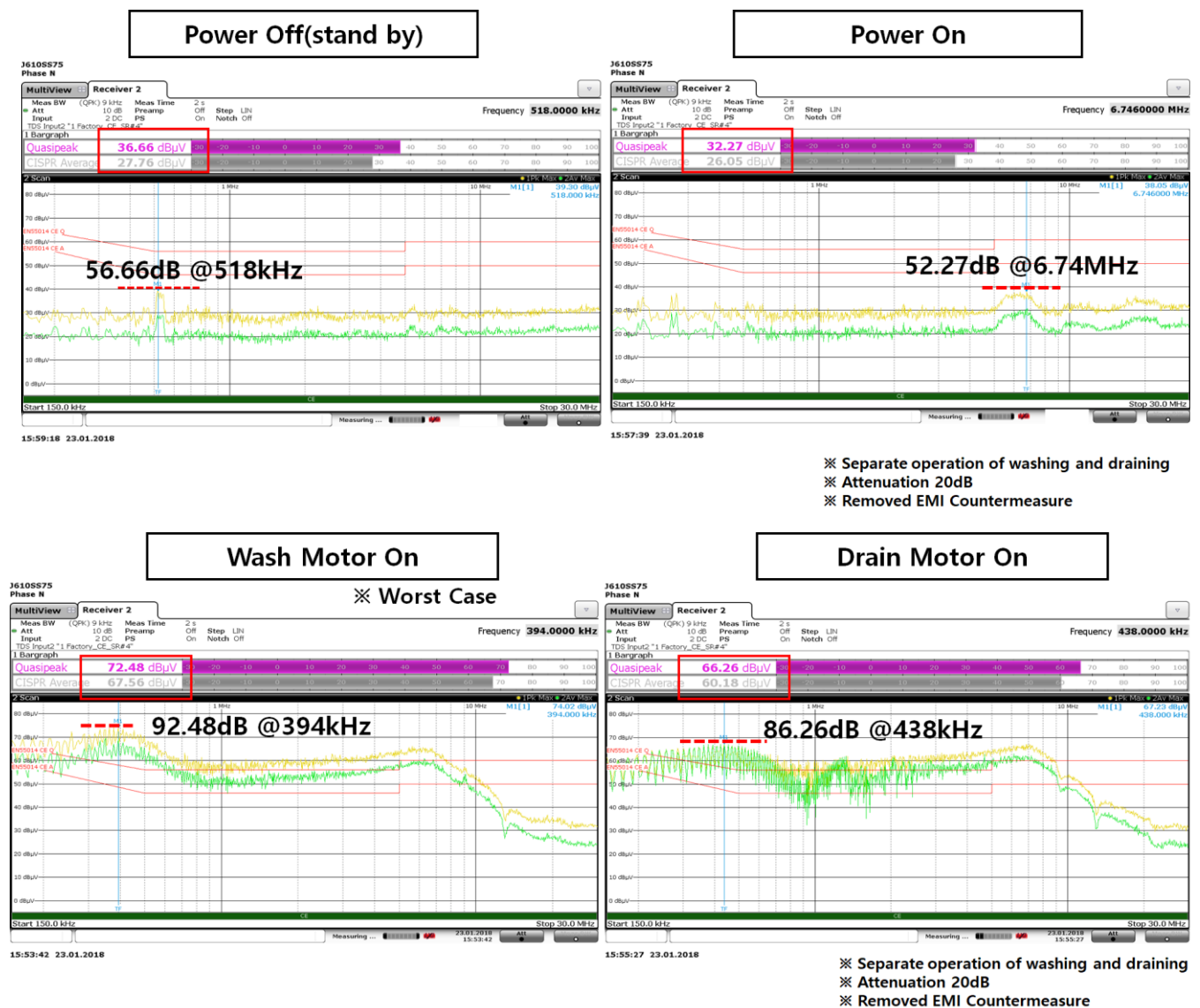


Figure 16. EMI (CE) results based on each load operation status.

As shown in Figure 19, the noise filter, power ground core, and washing motor core are the most effective in EMI improvement. The currently mass-produced noise filter components and individual external core components were modeled using the ANSYS designer tool, as depicted in Figure 20.

Based on the modeling data of individual components, we validated the modeling and attenuation characteristics of system components such as the washing motor and power input lines. The analysis of the attenuation characteristics of the noise filter depending on the presence of the motor and power lines is illustrated in Figure 21.



Figure 17. EMI (RP) results based on each load operation status.

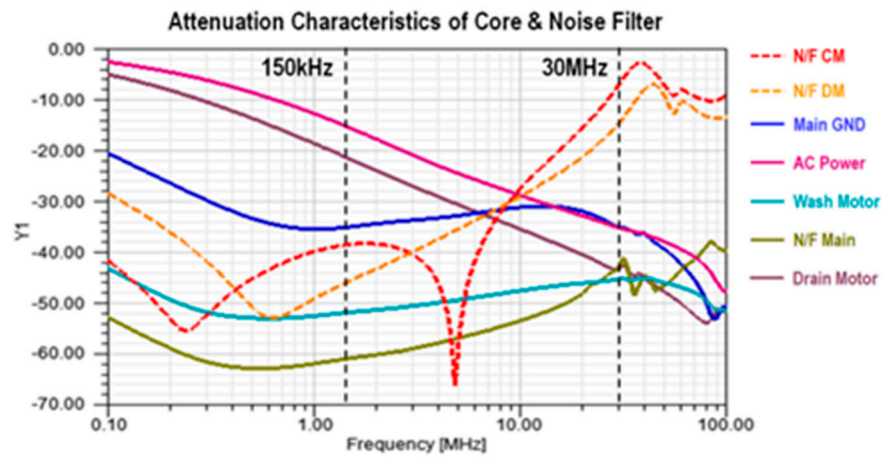


Figure 18. Harness core and noise filter attenuation characteristics.

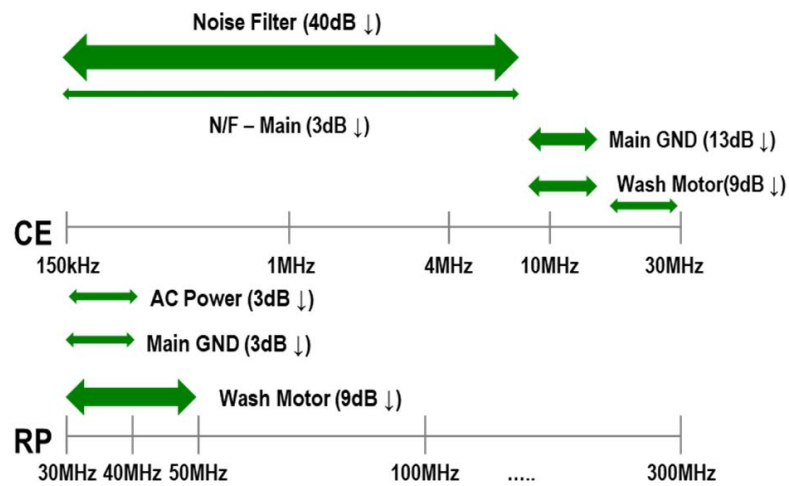


Figure 19. CE and RP suppression area for each harness core.

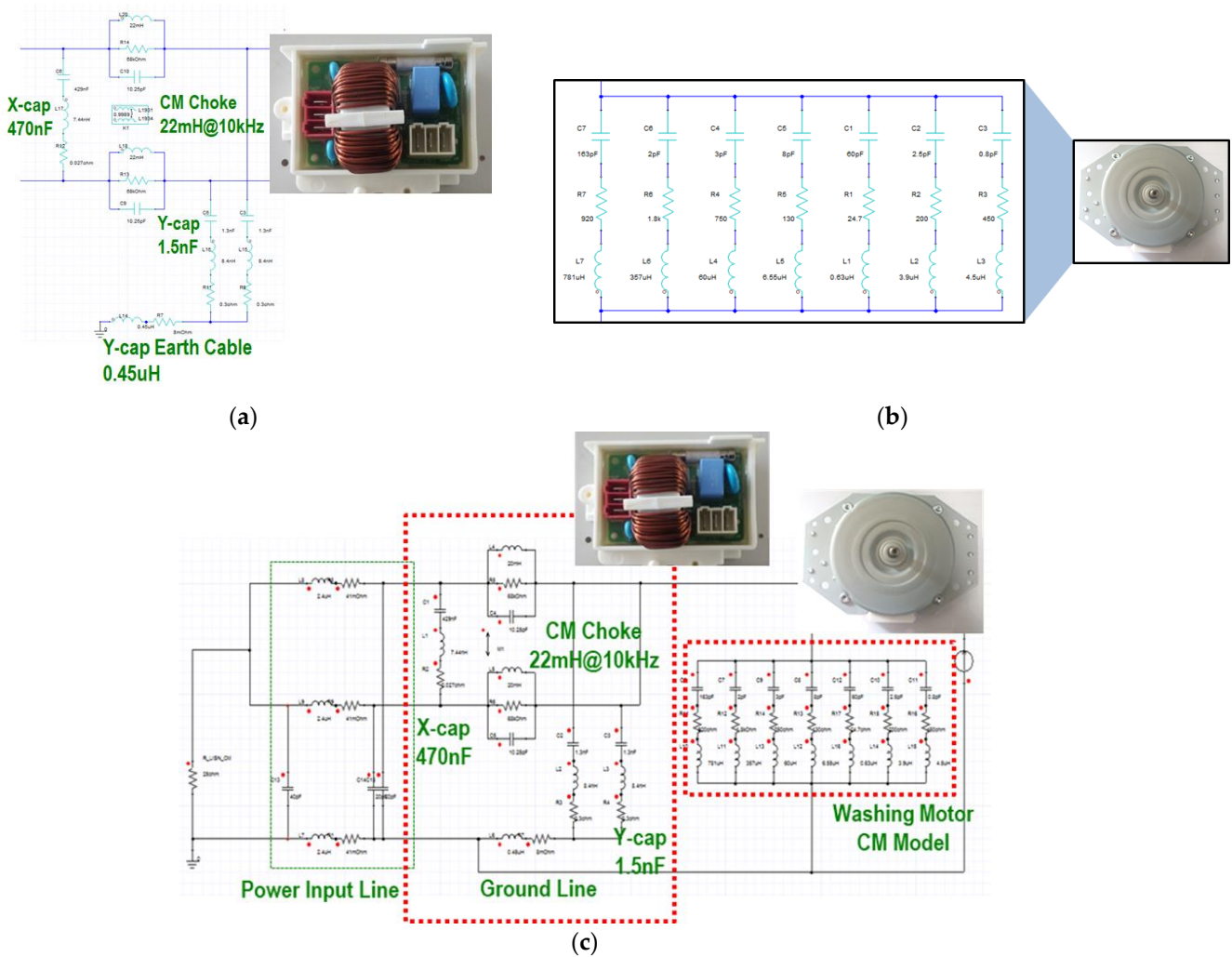


Figure 20. Circuit modeling of mass-produced noise filter components and individual external core components: (a) noise filter; (b) washing motor; (c) power input line.

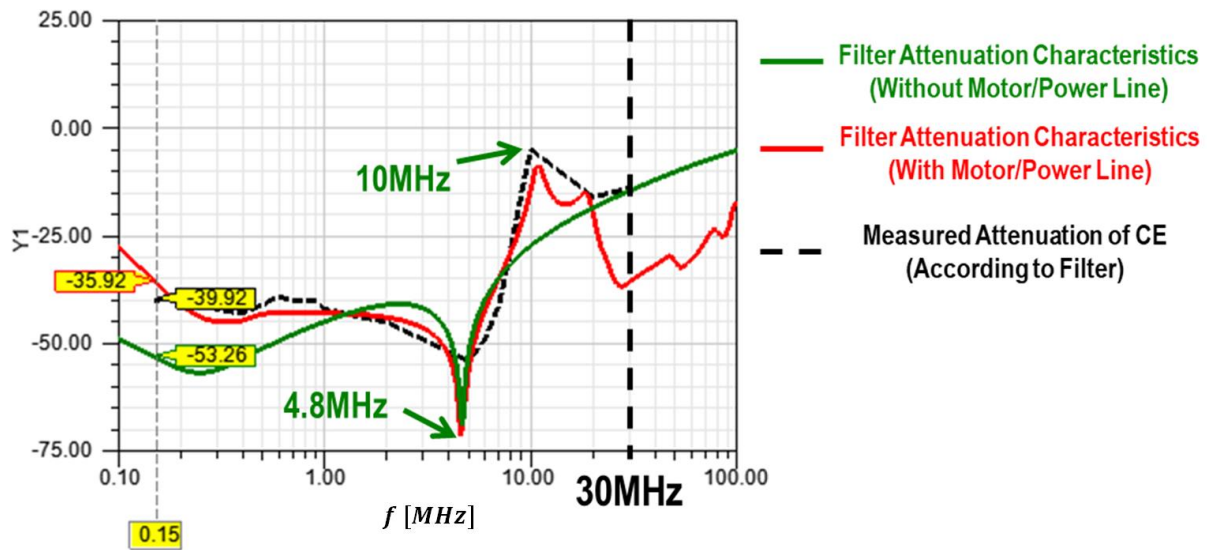


Figure 21. Attenuation characteristics of the noise filter.

### 3. Improved EMI Countermeasure Design

#### 3.1. EMI Countermeasure Design and Optimization

This subsection focuses on improving the noise generated by the washing motor, which has the most significant impact on the overall noise of the dishwasher, as shown in Figures 16 and 17. Examining Figure 22, it was determined that the washing motor resonates at 450 kHz, causing high-frequency components of the motor switching voltage to flow to ground through the motor case. This component was identified as noise due to common mode current. To minimize common mode current, the impedance of the three-phase core was optimized to be highest at 450 kHz, considering cost and size constraints.

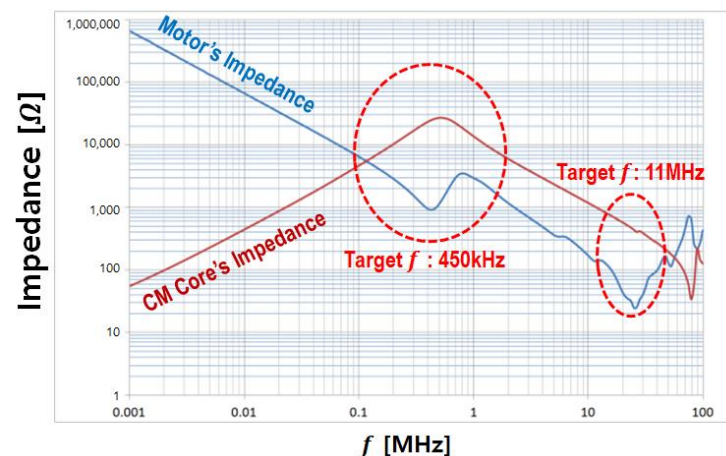


Figure 22. CM core and motor's impedance characteristics.

In particular, the ferrite core applied to the washing motor harness was mounted on the PCB for a structural change. When using a core on the harness, the insulation needs to be designed with thicker insulation to prevent wire insulation damage. As a result, even with a low number of turns for the same core size, the volume increases, and the maximum inductance is designed to be low. Therefore, when mounting the motor harness core on the PCB, enamel wires are wound directly on the core without the wire insulation, allowing an increase in the number of turns compared to the same-sized harness core. This increase in turns results in a higher maximum inductance. Due to cost considerations, the size and number of turns of the core were optimized by confirming the decision to mount it. The modified form of the harness core, changed from the actual product to a PCB type, can be observed in Figure 23.



Figure 23. Harness core changed to PCB mounting type.

The CE measurement results in Figure 24 are the results of testing after removing all ferrite cores applied to the harness except for the noise filter and applying the washing motor core [14,15]. The improved three-phase common mode core showed a significant improvement effect of over 20 dB at 450 kHz and had a margin of over 5 dB across the entire CE frequency range. Additionally, by examining Figure 25, it can be seen that the noise in the 30 MHz range of the RP band is reduced by more than 10 dBpW after the improvement.

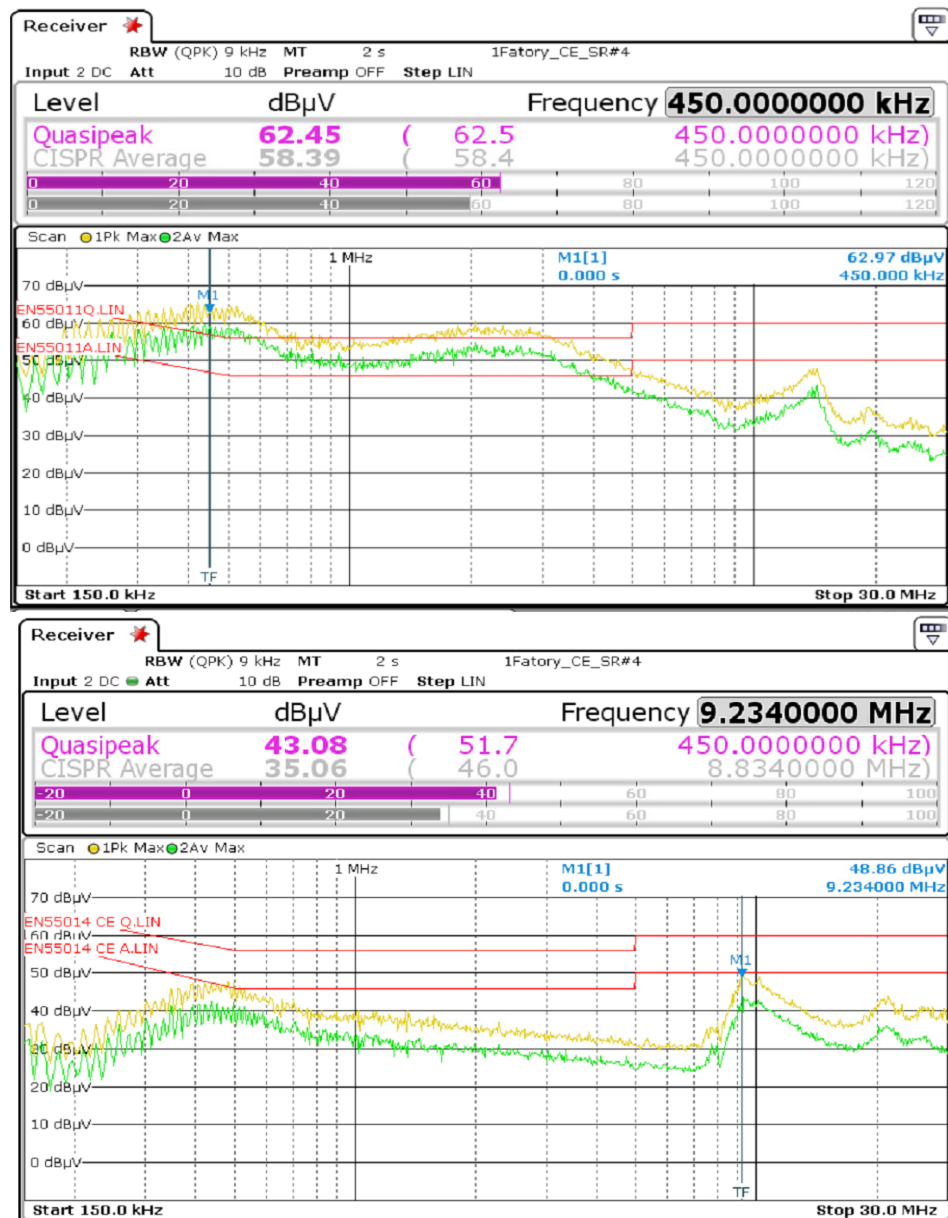


Figure 24. CE measurement results before and after applying the improved three-phase core.

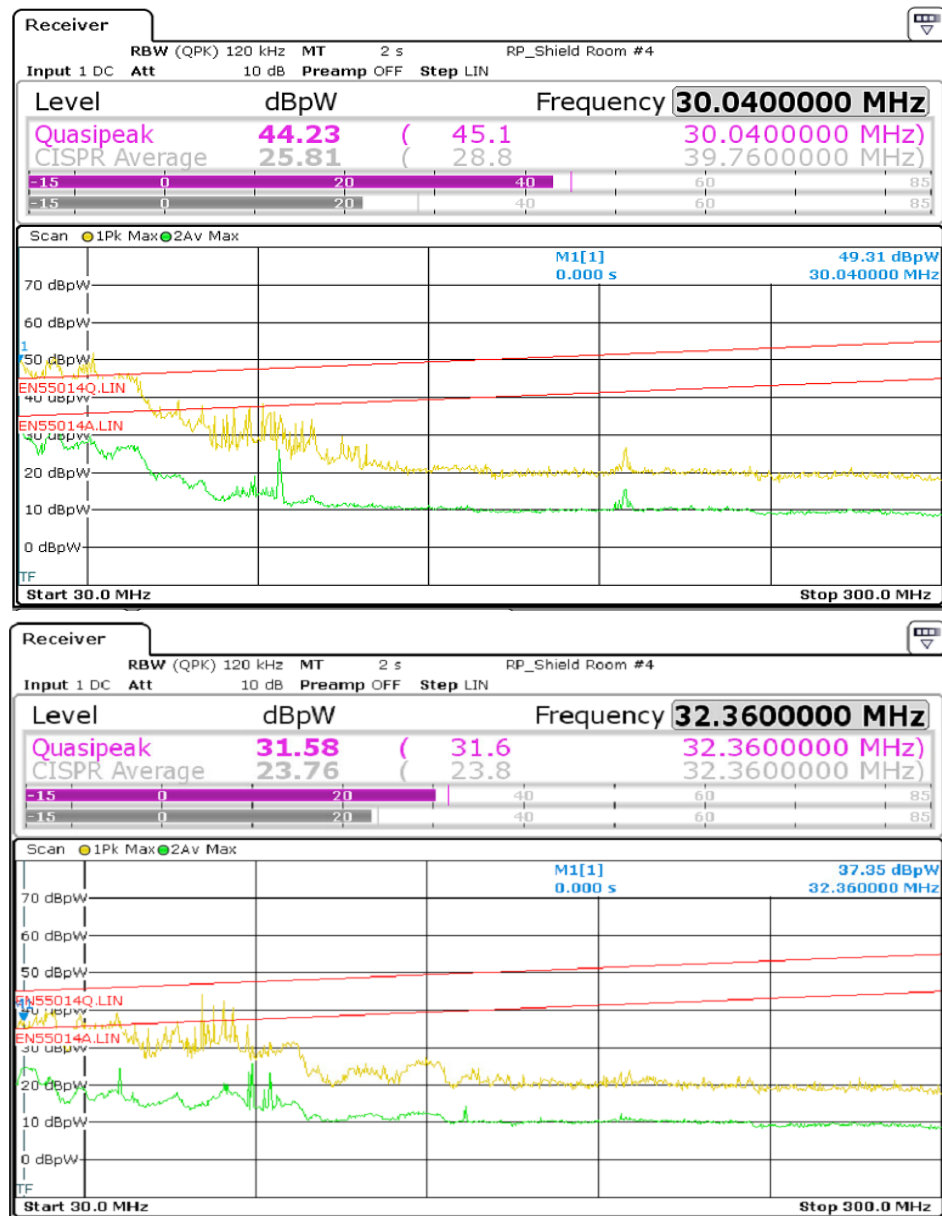


Figure 25. RP measurement results before and after applying the improved 3-phase core.

The improved three-phase core has reduced system noise across the CE and RP frequency ranges, prompting further consideration for lightweighting additional EMI mitigation components. Based on the earlier review results, all ferrite cores applied to the harness for CE improvement were removed. Additionally, a simulation was conducted to optimally design the noise filter, specifically, improving the performance of the CM core. The simulation results were then validated through experimentation.

To start, for lightweighting the noise filter CM core the diameter was reduced from 36Φ to 25Φ. After changing the core diameter, the initial noise filter’s CE noise characteristics are shown in Figure 26a. Through simulation, the filter was designed to have significant impedance at 250 kHz and 10 MHz. The improved noise filter with the CM core applied resulted in the characteristics shown in Figure 26b. Similarly, the RP noise characteristics, both initial and improved, are depicted in Figure 27a,b.

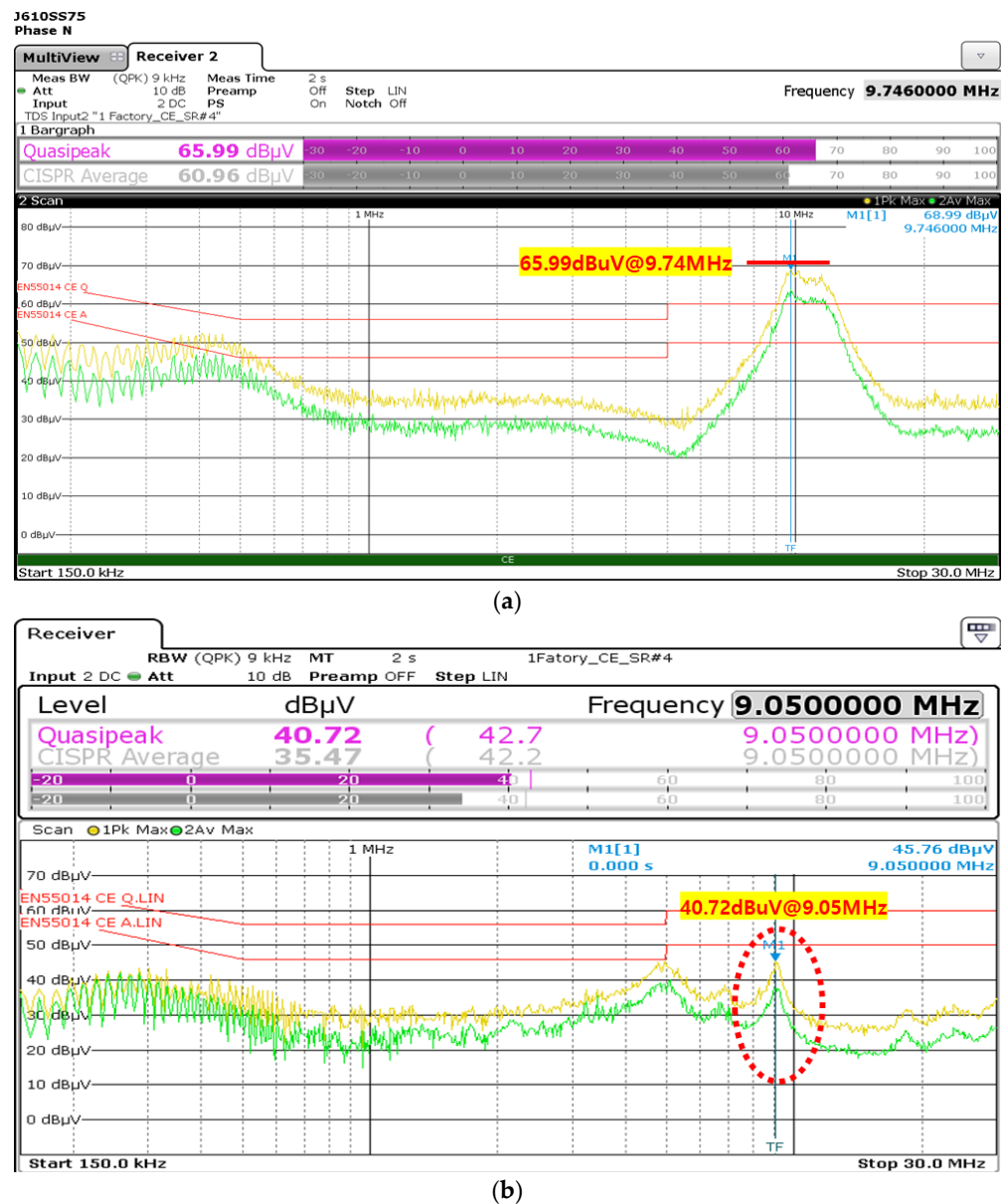
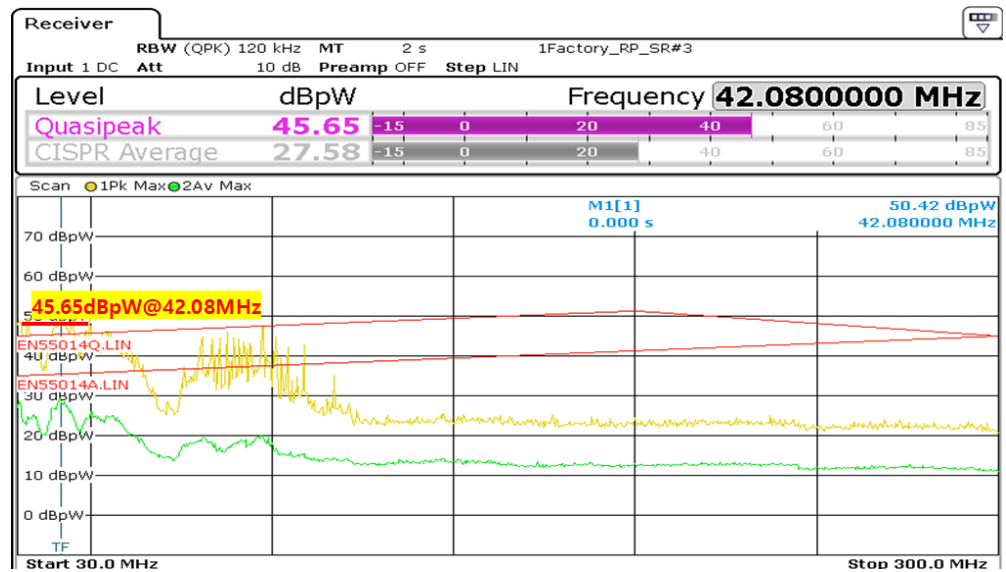


Figure 26. EMI (CE) measurement results: (a) before improvement; (b) after improvement.

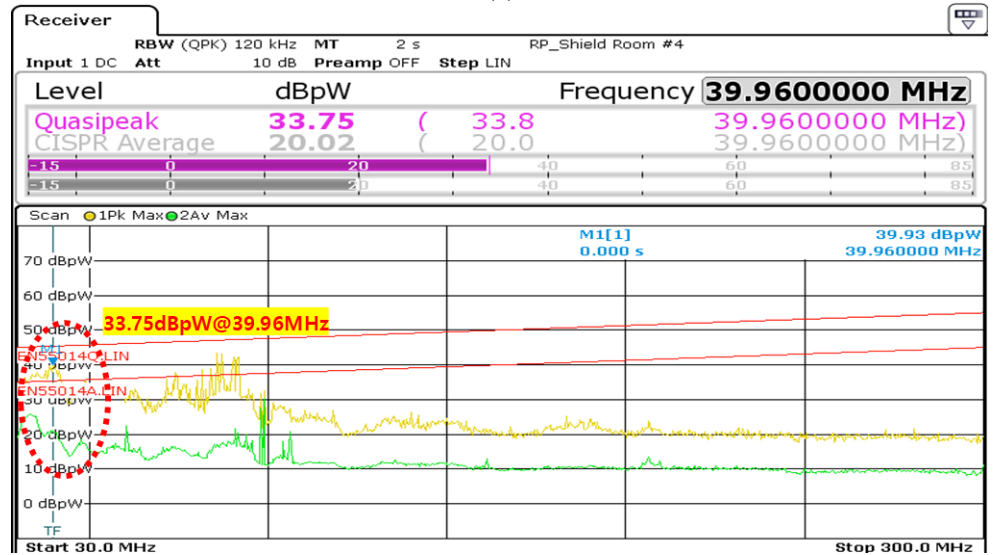
Meanwhile, the attenuation characteristics of the noise filter were compared with the existing measurement data, as shown in Figure 28 [16]. The system configuration with improved CE noise is illustrated in Figure 29. Additionally, the lightweighting of the noise filter CM core in the actual product can be observed in Figure 30.

In the case of CE, a clear improvement in noise was observed in the 300 kHz to 600 kHz range and at 10 MHz. Furthermore, a margin of more than 10 dBuV was secured compared to EMC standards (EN66014). The CE measurement results after the improvement are shown in Figure 21. Before improvement, the maximum value was approximately 65.99 dBuV at 9.74 MHz, but after improvement, it reached a maximum of 40.72 dBuV at 9.05 MHz [17–19].

For RP, a significant noise improvement was observed in the 40 MHz to 50 MHz range, and a margin of more than 5 dBpW was secured across the entire frequency range compared to the standard level (EN55014). The RP measurement results after the improvement are shown in Figure 22. Before improvement, the maximum value was approximately 45.65 dBpW at 42.08 MHz, but after improvement, it reached a maximum of 33.75 dBpW at 39.96 MHz [20,21].



(a)



(b)

Figure 27. EMI (RP) measurement results: (a) before improvement; (b) after improvement.

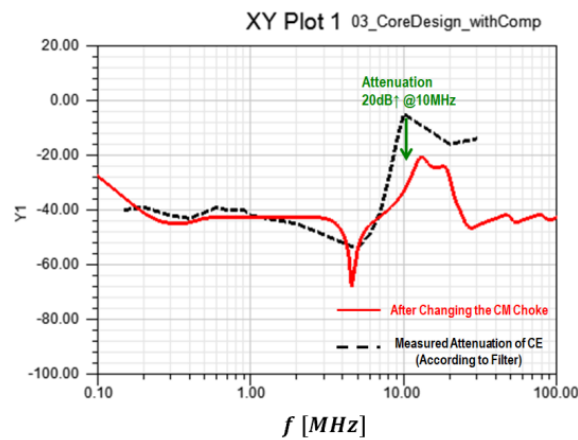
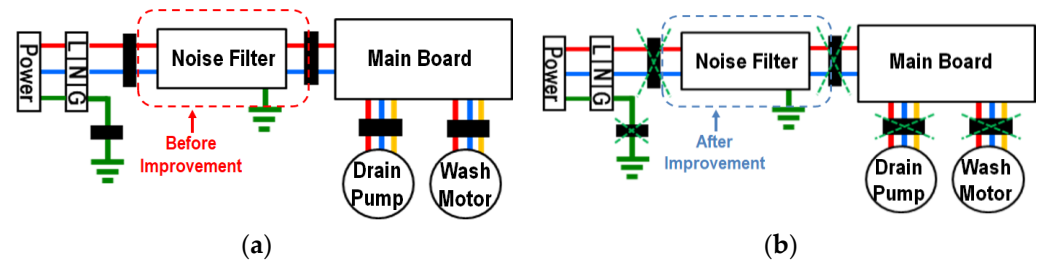
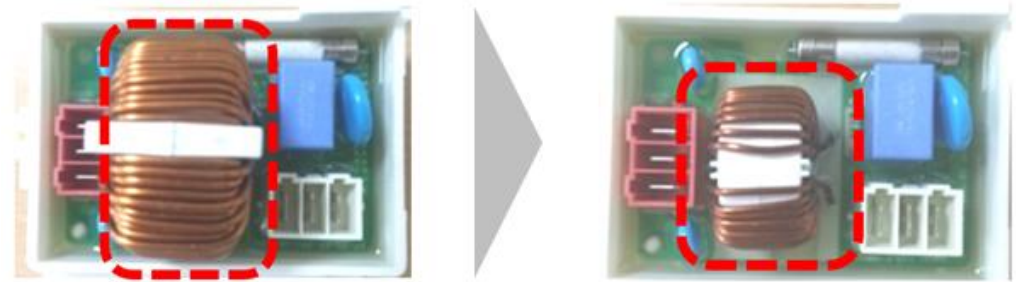


Figure 28. Comparison of measurements with noise filter simulation.



**Figure 29.** System configuration with applied noise filter improvement: (a) before improvement; (b) after improvement.



**Figure 30.** Noise filter CM core before and after lightweighting.

### 3.2. Verification of Improved EMI Countermeasures

The reverse function of the improved EMI countermeasure design was verified. This was performed through a temperature rise test on the main PCB Ass’y, which includes the noise filter with changed specifications and additional components. As shown in Table 3, the test was conducted under ambient temperature conditions of 25 °C. The results confirmed a margin of more than 20 °C compared to the component temperature specification (85 °C) [22].

**Table 3.** Test result of temperature of parts.

Part	Temp. Mass Product (°C)	Temp. Improvement (°C)	Specification of Part (°C)
Noise Filter Core	62.9	62	60
Motor CM Core	-	40	85 °C @25 °C

Additionally, as shown in Table 4, we conducted verification of the motor drive performance and protection logic based on the change in inductance due to the assembly of the built-in washing motor CM core PCB.

**Table 4.** Review list of adverse effects due to increased inductance.

Classification	Category	Description	Note
Washing Motor	Product detection logic settings	Review Behavior by RPM	Peak Component due to Instability
		Sensorless Switchover Failure Detected	Process Capability Analysis
		Sensorless Speed Divergence Detection	Within the Speed Limit
Drain Motor	Controller	Check Maximum Output	Equivalent Level of Mass Production
		Water Load → No Load	Peak Component due to Instability
		Sensorless Angle Instability Detection	Process Capability Analysis
		Sensorless Switchover Failure Detected	Process Capability Analysis
Product	Product detection logic settings	Sensorless Speed Divergence Detection	Within the Speed Limit
		Drain Completion Review	Test
		Foam Detection Review	Test

#### 4. Conclusions

This paper investigates the current noise levels of EMI in a dishwashing machine by measuring the noise levels under the baseline condition without harness cores and noise filters. Under the baseline condition, it was identified that the most critical noise component in common mode (CM) occurred during the operation of the washing motor, with a level of 101 dBuV at 362 kHz. To address this issue, an impedance analyzer was employed to analyze the impedance of the load (washing motor). The analysis revealed an impedance resonance in the frequency range of 300 kHz to 450 kHz, corresponding to the bandwidth where significant noise was generated. It was determined that CM noise flowed through the washing motor in this frequency range. As a solution, a core with significant impedance at 300 kHz was designed for the three-phase output of the washing motor, resulting in an improvement of over 20 dB in the 300 kHz range. The positive effect of the three-phase core led to a reduction in overall system noise, allowing for further lightweighting of the noise filter. Subsequently, a noise filter and system simulation were designed and validated through experiments. In conclusion, a margin of over 5 dB was achieved for both conducted emission (CE) and radiated power (RP) across the entire frequency range. Based on the key findings of this study, all cores connected to the product's harness were removed, and the CM choke inductance inside the noise filter was reduced from 18 mH to 11 mH, resulting in compactness and cost savings.

**Author Contributions:** Conceptualization, S.L. and T.K.; methodology, S.L.; validation, S.L. and C.J.; investigation, S.L. and C.J.; writing—original draft preparation, S.L. and C.J.; writing—review and editing, S.L. and C.J.; visualization, S.L. and C.J.; supervision, T.K. All authors have read and agreed to the published version of the manuscript.

**Funding:** This research received no external funding.

**Data Availability Statement:** Data are contained within the article.

**Conflicts of Interest:** The authors declare no conflict of interest.

#### References

1. Chung, Y. EMI/EMC Concepts and Regulatory Trends. *J. Korean Inst. Electron. Inf. Eng.* **1996**, *23*, 61–74.
2. Kim, C. Currents Status of EMC countermeasure technology. *J. Korean Inst. Electromagn. Eng. Sci.* **2010**, 73–79.
3. Paul, C. A Comparison of Common Mode and Differential-Mode Currents in Radiated Emission. *IEEE Trans. EMC* **1989**, *31*, 189–193. [[CrossRef](#)]
4. Ott, H.W. *Electromagnetic Compatibility Engineering*; John Wiley & Sons, Inc.: Hoboken, NJ, USA, 2008.
5. Nagrial, M.H.; Hellany, A. EMI/EMC Issue in Switch Mode Power Supplies. In Proceedings of the International Conference and Exhibition on Electromagnetic Compatibility, 1999, EMC York 99, York, UK, 12–13 July 1999; Conference Publication No. 464.
6. Skibinski, G.L.; Kerkman, R.J.; Schlegel, D. EMI Emissions of Modern PWM ac Drives. *Ind. Appl. Mag. IEEE* **1999**, *5*, 47–80. [[CrossRef](#)]
7. Jung, J.-C. EMI Analysis and Solution for Low Power Switching Power Supply. *Trans. Korean Inst. Power Electron.* **2001**, *6*, 141–148.
8. David, M. *A Handbook for EMC Testing and Measurement*; IET: London, UK, 1994.
9. Clayton, R.P. *Introduction to Electromagnetic Compatibility*, 2nd ed.; John Wiley & Sons, Inc.: Hoboken, NJ, USA, 2005.
10. Gonzalez, D.; Gago, J.; Balcells, J. Analysis and Simulation of Conducted EMI Generated by Switched Power Converters: Application to a Voltage Source Inverter. In Proceedings of the 2002 IEEE International Symposium on Industrial Electronics, ISIE 2002, L'Aquila, Italy, 26–29 May 2002; Volume 3, pp. 801–806.
11. Murai, Y.; Kubota, T.; Kawase, Y. Leakage current reduction for a high-frequency carrier inverter feeding an induction motor. *IEEE Trans. Ind. Appl.* **1992**, *28*, 858–863. [[CrossRef](#)]
12. Ott, H.W. Digital Circuit Grounding and Interconnection. In Proceedings of the IEEE International Symposium on Electromagnetic Compatibility, Boulder, CO, USA, 18–20 August 1981.
13. Vidmar, G.; Miljavec, D. A Universal High-Frequency Three-Phase Electric-Motor Model Suitable for the Delta- and Star-Winding Connections. *IEEE Trans. Power Electron.* **2015**, *30*, 4365–4376. [[CrossRef](#)]
14. Richard, L. *EMI Filter Design*; Marcel Dekker, Inc.: New York, NY, USA, 1996; pp. 56–100.
15. Montrose, M.I. *EMC and the Printed Circuit Board*; John Wiley & Sons, Inc.: Chichester, UK, 1998.
16. Ott, H.W. *Noise Reduction Techniques in Electronic System*; John Wiley & Sons, Inc.: Hoboken, NJ, USA, 2009.

17. Chen, H.; Hu, Y.; Wang, L.; Zhang, Z.; Chen, G. EMI filter design based on high-frequency modeling of common mode chokes. In Proceedings of the IEEE 27th International Symposium on Industrial Electronics (ISIE), Cairns, Australia, 13–15 June 2018; pp. 384–388.
18. Chand, B.; Kut, T.; Dickmann, S. Optimal design of active EMC filters. *Adv. Radio Sci.* **2013**, *11*, 243–249. [[CrossRef](#)]
19. Nave, M.J. *Power Line Filter Design for Switched—Mode Power Supplies*; Van Nostrand Reinhold: New York, NY, USA, 1991.
20. Drewniak, J.L.; Sha, F.; Hubing, T.H.; VanDoren, T.P.; Shaw, J. Diagnosing and Modeling Common-mode Radiation from Printed Circuit Boards with Attached Cables. In Proceedings of the 1995 IEEE International Symposium on Electromagnetic Compatibility, Chicago, IL, USA, 14–18 August 1995; pp. 465–470.
21. Lin, F.; Chen, D.Y. Reduction of Power Supply EMI Emission by Switching Frequency Modulation. *IEEE Trans. Power Electron.* **1994**, *9*, 132–137.
22. Mainali, K.; Oruganti, R. Conducted EMI mitigation techniques for switch-mode power converters: A survey. *IEEE Trans. Power Electron.* **2010**, *25*, 2344–2356. [[CrossRef](#)]

**Disclaimer/Publisher’s Note:** The statements, opinions and data contained in all publications are solely those of the individual author(s) and contributor(s) and not of MDPI and/or the editor(s). MDPI and/or the editor(s) disclaim responsibility for any injury to people or property resulting from any ideas, methods, instructions or products referred to in the content.